International Journal of Mass Spectrometry 448 (2020) 116261

Contents lists available at ScienceDirect

International Journal of Mass Spectrometry

journal homepage: www.elsevier.com/locate/ijms

Power series expansion of axially symmetric toroidal harmonics for toroidal ion trap

Appala Naidu Kotana [a], Atanu K. Mohanty [b, *]

[a] Department of Mathematics, Government Degree College, Pattikonda, Kurnool, 518380, Andhra Pradesh, India
[b] Department of Instrumentation and Applied Physics, Indian Institute of Science, Bangalore, 560012, Karnataka, India

ARTICLE INFO

Article history:
Received 17 August 2019
Received in revised form
10 November 2019
Accepted 15 November 2019
Available online 21 November 2019

Keywords:
Toroidal ion trap
Toroidal harmonic
Toroidal multipole coefficient
Three-term recurrence relation
Power series

ABSTRACT

This study presents a method to obtain power series expansions of toroidal harmonics in terms of radial and axial distances from the trapping circle. In order to obtain the power series expansion of individual toroidal harmonics, three-term recurrence relations are derived, which involve toroidal harmonics of order $n-1$, n, $n+1$ and derivative of toroidal harmonic of order n. Using these three-term recurrence relations a systematic procedure is presented to obtain the power series expansion for a toroidal harmonic of arbitrary order, up to the desired number of terms. With this procedure, the power series expansions of toroidal harmonics till order 5 are presented.

Verification of this theory was carried out on an arbitrary toroidal ion trap. The potential and the trajectory of a singly charged ion of 78 Th obtained by the power series were compared with those computed using the Boundary Element Method (BEM). The match was found to be very good.

1. Introduction

Toroidal ion traps are a new class of ion traps described in Ref. [1]. Toroidal ion traps consist of electrodes which are obtained by rotating cross-section of point trapping devices such as truncated Quadrupole Ion Trap (QIT) [2] or the Cylindrical Ion trap (CIT) [3] about an axis not passing through the trapping center.

In these devices, trapping occurs on a circle referred to as the trapping circle [4,5]. This is in contrast to the QIT and the CIT, in which trapping occurs at a point. Due to this difference in the trapping pattern, toroidal ion traps have advantages over QIT, such as having a larger trapping region and lower space charge effect [4].

Several experimental [1,6–14] and numerical [1,5,11,15–20] studies have been carried out on toroidal ion trap mass analysers with a variety of geometries. These geometries fall into three broad groups: the first group consists of curved electrodes such as hyperbolic surfaces or doughnut-shaped surfaces [1,4,6,7,10–13,15]; the second group consists of electrodes with flat cylindrical surfaces and annuli [8,15,20]; and the third group consists of planar electrodes [9,14].

In order to understand the working of toroidal ion traps, an analytical description of the potential is required. Because the trapping of ions occurs on a circle and not at a point, the spherical harmonics that are used to describe the potential in point trapping devices cannot be used for toroidal ion traps. It is for this reason that a new approach has been adopted in the literature to describe the potential using toroidal multipole expansion [16,19]. This expansion is in terms of toroidal harmonics and the coefficients of these harmonics are called toroidal multipole coefficients.

A recent study [5] has provided three numerical methods to evaluate the toroidal multipole coefficients. However, each term of this expansion is far more complex than the spherical multipole counterpart of point trapping devices [21]. While the terms of the spherical harmonic multipole expansion are polynomials, the toroidal harmonics are not polynomials. The toroidal harmonics vary in a complicated way in both the radial and axial directions. Further these harmonics do not provide an easy description of variation of potential terms of radial and axial distances as provided by spherical harmonics for point trapping devices.

The power series representation of potential in point trapping devices, such as the QIT and the CIT, enabled researchers to analyze potentials [3,21–23] and trapped ion dynamics due to field inhomogeneities [22,24–32]. The understanding of fields helped in trap design [3]. In contrast, the toroidal multipole expansion does not provide a similar description.

With this background, a power series expansion for each

* Corresponding author.
E-mail addresses: kotanaappalanaidu@gmail.com (A.N. Kotana), amohanty@iisc.ac.in (A.K. Mohanty).

https://doi.org/10.1016/j.ijms.2019.116261
1387-3806/

toroidal harmonic in terms of radial and axial distances from the trapping circle has been developed. With this, it is possible to obtain a power series expansion of the potential and fields as a function of the radial and axial distances from the trapping circle. The derivation presented here is elegant in that it is shown that the power series of higher order harmonics are all obtainable from the lowest order harmonic using three-term recurrence relations. The theory that has been developed in this paper has been numerically verified.

This paper has two principal contributions. The first is that it provides the relationship between toroidal harmonics of different orders. The second is that it provides a power series in a form that is particularly convenient for mass spectrometry.

As a caveat it is emphasized that this study is limited to the derivation of power series for describing potential and field inside the toroidal ion trap. Although the analysis of performance characteristics of a toroidal trap is not within the scope of the present study, a brief example of how these power series could be used to predict nonlinear resonance has been included to give a flavor of the possible applications of these power series.

Section 2 presents the computational methods used and in Section 3, the required theory is presented. Finally, the results are presented in Section 4.

2. Computational methods

2.1. Overview

To give an overview of the contribution of this study, Fig. 1 presents the steps that need to be taken to obtain the power series. These steps are briefly described below.

Steps 1, 2, and 3 are available in the literature. Step 4 will be discussed in Section 3, Theory below.

2.2. The boundary element method

The boundary element method is used for computing the potential and field at an arbitrary point. This method has been described in detail by Tallapragada et al. [35].

2.3. Trajectory computation

The equations of ion motion in the toroidal ion trap presented in this paper are non-linear coupled ordinary differential equations. These are difficult to solve analytically. The Runge-Kutta fourth order method (a numerical method) was used to solve the equations [37].

2.4. Determination of toroidal multipole coefficients

The potential in an arbitrary toroidal ion trap is modelled using an infinite series of toroidal harmonics. The coefficients in the series are called toroidal multipole coefficients. Three different methods have been reported to compute these multipole coefficients in Ref. [5]. In the present study, the SC-BEM method was used to obtain the toroidal multipole coefficients [5].

In order to compute the multipole coefficients, the trapping circle needs to be determined. This circle was obtained numerically by locating points within the trapping region at which field is zero. This was done using the Newton-Raphson method [36].

2.5. Computation of mathieu parameters

The Mathieu parameters a_r and q_r, a_z and q_z are required to compute β_r and β_z [38,39]. These parameters β_r and β_z are useful in describing regions of non-linearities in the stability plot of a given toroidal trap [18].

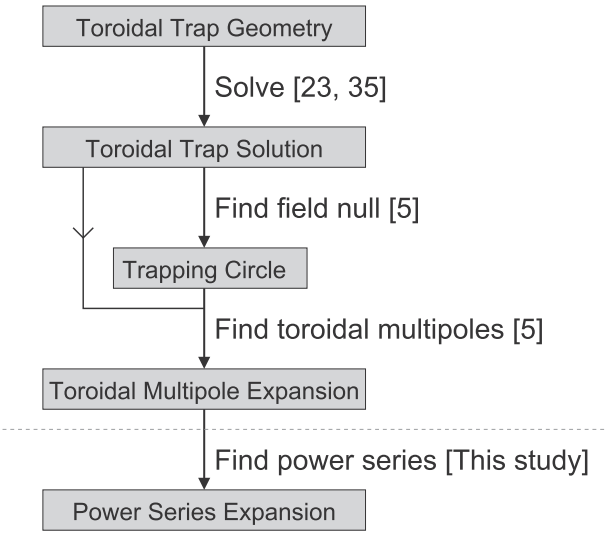

Fig. 1. Steps involved in obtaining power series expansion.

1. Solution of the Laplace equation: Given any toroidal trap geometry, a Laplace equation solver is used to compute potential and field within the trap with a given set of applied potentials. This solver could use the Finite Difference Method (FDM) eg. SIMION [33], the Finite Element Method (FEM) eg. ANSYS [34], or the Boundary Element Method (BEM) [23,35]. In the present study, a BEM package developed in-house has been used.
2. Determination of the trapping circle: Having the ability to compute the field, the next step is to find where the field is zero. This is done numerically. In the present study a two-dimensional Newton-Raphson method [36] is used. The circle perpendicular to the axis of rotational symmetry of the toroidal ion trap, and passing through the zero-field point, is called the trapping circle and is used as the reference circle for the toroidal multipole expansion [5].
3. Determination of the multipole expansion: The next step is to obtain the toroidal multipole expansion. This can be obtained using any one of the methods outlined in Ref. [5].
4. Determination of the power series expansion: This is the main contribution of the present study. Given the multipole expansion it provides a power series expansion of the potential in terms of radial and axial distances from the trapping circle.

The parameters a_r and q_r are related to the radial direction ion motion; a_z and q_z are related to the axial direction ion motion. These are computed using the following formulae [18].[1]

$$a_r = \frac{4eU_{dc}\lambda_1}{m\Omega^2} \tag{1}$$

$$q_r = -\frac{2eV_{rf}\lambda_1}{m\Omega^2} \tag{2}$$

$$a_z = -a_r \tag{3}$$

$$q_z = -q_r, \tag{4}$$

where U_{dc} is d.c. potential, V_{rf} is amplitude of r.f. potential and Ω is angular frequency of r.f. potential applied to the trap electrodes. The value of λ_1 in Eqs. (1) and (2) is given by

[1] The details of derivation of these parameters are discussed Ref. [5].

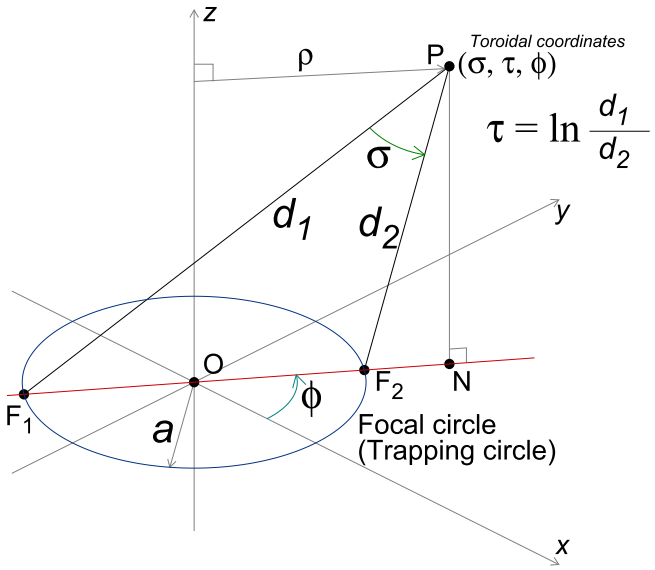

Fig. 2. Toroidal coordinates system. $P(x,y,z)$ is an arbitrary point in the Cartesian coordinate system. O is the origin and, the projection of P in the radial plane is denoted by N [5].

$$\lambda_1 = \frac{3\pi}{16a^2\sqrt{2}}\sqrt{(2a_0 - a_2)^2 + b_2^2}, \tag{5}$$

where a is radius of the trapping circle; a_0, a_2 and b_2 are the toroidal multipole coefficients [5].

3. Theory

This section presents the theory developed to express the potential within the toroidal ion trap in the form of power series. This will be used to derive equations of ion motion in toroidal ion trap.

Since this section is lengthy, it has been divided into several subsections. These include 3.1 Toroidal harmonics, 3.2 Three-term recurrence relations for toroidal harmonics, 3.3 Power series expansion for the lowest order toroidal harmonic T_0, and 3.4 Power series expansion of toroidal harmonics T_1 through T_5 and U_1 through U_5. Finally, Power series expansion for describing the potential inside a toroidal ion trap and Equations of ion motion in the toroidal ion trap will be presented in Sections 3.5 and 3.6, respectively.

3.1. Toroidal harmonics

A schematic view of the toroidal coordinate system [40] is shown in Fig. 2. An arbitrary point in the toroidal coordinate system is denoted by $P(\sigma,\tau,\varphi)$. The reference circle[2] of radius a, shown in the radial plane of this figure, is the focal circle. The line passing through the origin and the projection of point P on the radial plane intersects the focal circle at two different points F_1 and F_2. The longest distance PF_1 from P is defined to be d_1 and the shortest distance PF_2 from P is defined as d_2. The parameter τ is defined as $\log\left(\frac{d_1}{d_2}\right)$, and σ is defined by the angle between PF_1 and PF_2. The angle ϕ is defined to be the angle subtended with the x-axis by the line joining the origin and the projection of P in the radial plane. The distance of the projection of P on the radial plane from the origin is denoted by ρ and is given by $\rho = \sqrt{x^2+y^2}$. It is to be noted that in the mass spectrometry literature what is denoted ρ here is denoted by r. We used r in all geometry diagrams, however to be consistent with mathematical text books [40,41] we use ρ in our derivations and reserve the symbol r for the distance from the origin. The toroidal coordinates and Cartesian coordinates are related by $x = a\frac{\sinh\tau}{\cosh\tau-\cos\sigma}\cos\varphi$, $y = a\frac{\sinh\tau}{\cosh\tau-\cos\sigma}\sin\varphi$, $z = a\frac{\sin\sigma}{\cosh\tau-\cos\sigma}$ and $\rho = a\frac{\sinh\tau}{\cosh\tau-\cos\sigma}$ [40].

As mentioned earlier, the trapping of ions in toroidal traps occurs on a circle. This circle is considered as the focal circle for the toroidal coordinate system. Usually this circle lies on the radial plane. However, for some geometries, it may have an offset z_c from the radial plane. In such cases, the coordinate system will be shifted in the z-direction by z_c so that the offset will be zero; that is, in the shifted system, the variable z will be changed to $z - z_c$. For simplicity, z_c was suppressed in some of our derivations. However, in the final result z has been replaced by $z - z_c$.

In the toroidal coordinate system, the following relations can be derived with the help of the diagram shown in Fig. 2

$$d_1 = \sqrt{(\rho+a)^2 + (z-z_c)^2} \tag{6}$$

$$d_2 = \sqrt{(\rho-a)^2 + (z-z_c)^2} \tag{7}$$

$$\cos\sigma = \frac{d_1^2 + d_2^2 - 4a^2}{2d_1d_2} \tag{8}$$

$$\sin\sigma = \frac{2a(z-z_c)}{d_1d_2} \tag{9}$$

where a is radius of the trapping circle and z_c is height of the trapping circle from the radial plane.

The governing equation for the potential in toroidal ion trap is the Laplace equation $\nabla^2\Psi = 0$. In toroidal coordinate system this equation is given by Refs. [40,41]

$$\sinh\tau\frac{\partial}{\partial\sigma}\left(\frac{1}{\cosh\tau-\cos\sigma}\frac{\partial\Psi}{\partial\sigma}\right) + \frac{\partial}{\partial\tau}\left(\frac{\sinh\tau}{\cosh\tau-\cos\sigma}\frac{\partial\Psi}{\partial\tau}\right) + \frac{1}{\sinh\tau(\cosh\tau-\cos\sigma)}\frac{\partial^2\Psi}{\partial\varphi^2} = 0 \tag{10}$$

For toroidal ion traps, the potential Ψ is axially symmetric, that is it is independent of φ. Separable solutions of the axially symmetric Laplace equation that are suitable for toroidal traps are given by Refs. [40,41]

$$T_n(\sigma,\tau) = \sqrt{\cosh\tau-\cos\sigma}\cos(n\sigma)Q_{n-\frac{1}{2}}(\cosh\tau) \tag{11}$$

$$U_n(\sigma,\tau) = \sqrt{\cosh\tau-\cos\sigma}\sin(n\sigma)Q_{n-\frac{1}{2}}(\cosh\tau) \tag{12}$$

where n is a non negative integer and $Q_{n-\frac{1}{2}}(\cosh\tau)$ is associated Legendre function. These functions, T_n and U_n, are called the toroidal harmonics [16,19].

The potential in an arbitrary toroidal ion trap mass analyser can be described as linear combination of toroidal harmonics as follows:

$$\Psi = a_0T_0 + \sum_{n=1}^{\infty}[a_nT_n + b_nU_n] \tag{13}$$

where a_n and b_n are the toroidal multipole coefficients [19].

[2] In the context of toroidal ion traps the trapping circle is used as the reference circle.

3.2. Three-term recurrence relations for toroidal harmonics

A method to obtain the power series expansion of arbitrary toroidal harmonics is presented here.

It is observed that if W is an axially symmetric solution to the Laplace equation then $\frac{\partial W}{\partial z}$ and $\left(\rho\frac{\partial}{\partial\rho}+z\frac{\partial}{\partial z}\right)W$ are also axially symmetric solutions to the Laplace equation. A brief discussion on how these observations are obtained is given in Appendix A.1. This was used as a means for generating new solutions from existing solutions. Each toroidal harmonic is a solution to the axially symmetric Laplace equation; on applying the operators $\frac{\partial}{\partial z}$ and $\left(\rho\frac{\partial}{\partial\rho}+z\frac{\partial}{\partial z}\right)$ on it, these also have to be solutions, and they should be some linear combination of toroidal harmonics.

Using the above properties the following novel relations are obtained. An outline of derivations of these relations is presented in Appendix A. These relations will be used to obtain the expansions of all higher order harmonics from the expansion of simplest harmonic T_0.

$$\frac{\partial T_0}{\partial z} = -\frac{1}{2a}U_1 \tag{14}$$

$$\left(\rho\frac{\partial}{\partial\rho}+z\frac{\partial}{\partial z}\right)T_0 = -\frac{1}{2}(T_0+T_1) \tag{15}$$

$$\left(\rho\frac{\partial}{\partial\rho}+z\frac{\partial}{\partial z}\right)T_n = \frac{n-\frac{1}{2}}{2}T_{n-1}-\frac{T_n}{2}-\frac{n+\frac{1}{2}}{2}T_{n+1} \tag{16}$$

$$\left(\rho\frac{\partial}{\partial\rho}+z\frac{\partial}{\partial z}\right)U_n = \frac{n-\frac{1}{2}}{2}U_{n-1}-\frac{U_n}{2}-\frac{n+\frac{1}{2}}{2}U_{n+1} \tag{17}$$

where T_n and U_n are toroidal harmonics of order n. It should be noted that these quantities (T_0, T_n and U_n) denote the toroidal harmonics and not just specific parts such as the Legendre functions.

Fig. 3 shows the trapping circle for an arbitrary trap without showing the trap electrodes. In this diagram, a indicates radius of the trapping circle, z_c is the trapping height from the radial plane

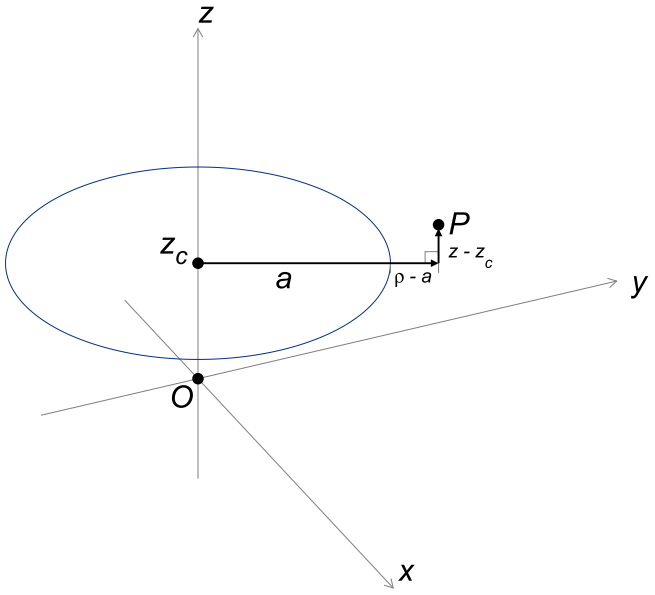

Fig. 3. Depiction of the radial distance $\rho - a$ and axial distance $z - z_c$ of an arbitrary point P from the trapping center. These distances are normalized as $u = \frac{\rho-a}{2a}$ and $v = \frac{z-z_c}{2a}$ to obtain the power series of toroidal harmonics in a convenient form.

and P is an arbitrary point in the trapping region. Also, the radial and axial distances of P from the trapping circle are indicated by $\rho - a$ and $z - z_c$. In terms of these distances, the variation of the field in the toroidal trap is not well understood. A simple power series expansion of potential in terms of these distances will give a better understanding of the fields. The power series expansion of potential is obtained by substitution of the power series of individual toroidal harmonics in the multipole expansion. The power series expansions of toroidal harmonics are computed in terms of these distances. In order to obtain the power series of the toroidal harmonics in convenient form, normalized distances from the trapping center as defined by

$$u = \frac{\rho-a}{2a}, \tag{18}$$

$$v = \frac{z-z_c}{2a}, \tag{19}$$

were used.

The axially symmetric Laplace equation in terms of variables u and v for axially symmetric problems is given by

$$\frac{\partial\psi}{\partial u}+u\left(\frac{\partial^2\psi}{\partial u^2}+\frac{\partial^2\psi}{\partial v^2}\right)+\frac{1}{2}\left(\frac{\partial^2\psi}{\partial u^2}+\frac{\partial^2\psi}{\partial v^2}\right)=0 \tag{20}$$

The derivative operators $\frac{\partial}{\partial z}$ and $\rho\frac{\partial}{\partial\rho}+z\frac{\partial}{\partial z}$ with normalized distances take the following form:

$$\frac{\partial}{\partial z} = \frac{1}{2a}\frac{\partial}{\partial v} \tag{21}$$

$$\rho\frac{\partial}{\partial\rho}+z\frac{\partial}{\partial z} = \frac{1}{2}\frac{\partial}{\partial u}+u\frac{\partial}{\partial u}+v\frac{\partial}{\partial v} \tag{22}$$

Using these relations, the equations from Eqs. (14)–(17) will take the following from:

$$\frac{\partial T_0}{\partial v} = -U_1 \tag{23}$$

$$\left(\frac{1}{2}\frac{\partial}{\partial u}+u\frac{\partial}{\partial u}+v\frac{\partial}{\partial v}\right)T_0 = -\frac{1}{2}(T_0+T_1) \tag{24}$$

$$\left(\frac{1}{2}\frac{\partial}{\partial u}+u\frac{\partial}{\partial u}+v\frac{\partial}{\partial v}\right)T_n = \frac{n-\frac{1}{2}}{2}T_{n-1}-\frac{T_n}{2}-\frac{n+\frac{1}{2}}{2}T_{n+1} \tag{25}$$

$$\left(\frac{1}{2}\frac{\partial}{\partial u}+u\frac{\partial}{\partial u}+v\frac{\partial}{\partial v}\right)U_n = \frac{n-\frac{1}{2}}{2}U_{n-1}-\frac{U_n}{2}-\frac{n+\frac{1}{2}}{2}U_{n+1} \tag{26}$$

For easy referencing, Eq. (23) is called as " U_1 Eq", Eq. (24) is called as " T_1 Eq", Eq. (25) is called as " T_n Eq" and Eq. (26) is called as " U_n Eq".

Using Eqs (23)–(26), it is possible to obtain the power series for all toroidal harmonics starting with the power series for T_0.

3.3. Power series expansion for the lowest order toroidal harmonic T_0

The toroidal harmonic $T_0 = \sqrt{\cosh\tau-\cos\sigma}Q_{-\frac{1}{2}}(\cosh\tau)$ can be written in terms of the complete elliptic integral of the first kind [5,42]. The simplification of T_0 in terms of the elliptic integral takes the form $T_0 = \sqrt{2}\,\frac{2a}{d_1}K\left(\frac{d_2}{d_1}\right)$ [5,42]. The expressions for d_1 and d_2 can be simplified in terms of normalized distances to obtain

$d_1 = \sqrt{1+2u+u^2+v^2}$ and $d_2 = \sqrt{u^2+v^2}$. Using these expressions, T_0 is further simplified to

$$T_0 = \sqrt{2}\ \frac{1}{\sqrt{1+2u+u^2+v^2}} K\left(\sqrt{\frac{u^2+v^2}{1+2u+u^2+v^2}}\right) \tag{27}$$

The power series expansion of the complete elliptic integral of first kind, $K(k)$, is known [42]. In principle, it is possible to obtain the power series of T_0 by multiplying the power series of the elliptic integral with the power series expansion of the radical.

However, a more efficient method has been developed in this study to compute the power series of T_0. In this method, the power series is obtained using recurrence relations between its coefficients.

Let the power series of a solution of the axially symmetric Laplace equation be

$$\psi(u,v) = \sum_{m=0}^{\infty}\sum_{n=0}^{\infty} C_{m,n} u^m v^n. \tag{28}$$

Substituting $\psi(u,v)$ from Eq. (28) in Eq. (20) and equating coefficients of $u^m v^n$ to zero will give the following recurrence relations.

$$C_{2,n} = -\frac{(n+1)(n+2)}{2} C_{0,n+2} - C_{1,n} \tag{29}$$

$$C_{m-1,n+2} + \frac{1}{2} C_{m,n+2} = -\frac{(m+1)^2}{(n+1)(n+2)}\left[C_{m+1,n} + \frac{m+2}{2(m+1)} C_{m+2,n}\right]; \quad \text{for } m > 2 \tag{30}$$

These recurrence relations for the coefficients of the power series are valid not only for T_0, but also for any other toroidal harmonic.

In order to obtain the power series for T_0, its $C_{0,n}$ and $C_{1,n}$ values are required for $n = 0, 1, 2, \ldots$. To obtain the $C_{0,n}$ values we note that

$$T_0(0,v) = \sqrt{2}\int_0^{\frac{\pi}{2}} \frac{1}{\sqrt{1+v^2\sin^2\theta}} d\theta = \sum_{n=0}^{\infty} C_{0,n} v^n$$

Expanding the integrand using the binomial theorem and integrating individual terms yields

$$C_{0,n} = \begin{cases} \dfrac{\pi}{\sqrt{2}} \dbinom{\frac{-1}{2}}{\frac{n}{2}} \dfrac{1}{2}\dfrac{3}{4}\cdots\dfrac{n-1}{n} & \text{for } n \text{ even} \\ 0 & \text{for } n \text{ odd} \end{cases} \tag{31}$$

Similarly, the values of $C_{1,n}$ can be obtained as

$$\left.\frac{\partial T_0(u,v)}{\partial u}\right|_{u=0} = -\sqrt{2}\int_0^{\frac{\pi}{2}} \frac{1}{\left[1+v^2\cos^2\theta\right]^{\frac{3}{2}}} d\theta = \sum_{n=0}^{\infty} C_{1,n} v^n$$

Expanding the integrand using the binomial theorem and integrating individual terms yields

$$C_{1,n} = \begin{cases} -\dfrac{\pi}{\sqrt{2}} \dbinom{\frac{-3}{2}}{\frac{n}{2}} \dfrac{1}{2}\dfrac{3}{4}\cdots\dfrac{n-1}{n} & \text{for } n \text{ even} \\ 0 & \text{for } n \text{ odd} \end{cases} \tag{32}$$

It is to be noted that from Eq. (31) and Eq. (32) the relation $C_{1,n} = -(n+1)C_{0,n}$ holds. Using this relation $C_{1,n}$ can be computed from $C_{0,n}$.

Once $C_{0,n}$ and $C_{1,n}$ are known $C_{2,n}$ can be computed using recurrence relation given in Eq. (29). $C_{0,n}$, $C_{1,n}$ and $C_{2,n}$ are used as the starting values in the recurrence relation Eq. (30) to obtain $C_{m,n}$. Thus the power series of T_0 can be obtained as:

$$T_0 = \frac{\pi}{\sqrt{2}}\left[1 - u + \frac{5}{4}u^2 - \frac{1}{4}v^2 - \frac{7}{4}u^3 + \frac{3}{4}uv^2 + \frac{169}{64}u^4 - \frac{51}{32}u^2v^2 + \frac{9}{64}v^4 - \frac{269}{64}u^5 + \frac{95}{32}u^3v^2 - \frac{45}{64}uv^4 + \ldots\right] \tag{33}$$

3.4. Power series expansion of toroidal harmonics T_1 through T_5 and U_1 through U_5

From " T_1 Eq" shown in Eq. (24), $T_1 = -T_0 - 2\left(\frac{1}{2}\frac{\partial}{\partial u} + u\frac{\partial}{\partial u} + v\frac{\partial}{\partial v}\right)T_0$. A substitution of the T_0 series in this gives T_1 series as follows:

$$T_1 = \frac{\pi}{\sqrt{2}}\left[\frac{1}{2}u - u^2 + \frac{1}{2}v^2 + \frac{27}{16}u^3 - \frac{33}{16}uv^2 - \frac{11}{4}u^4 + \frac{87}{16}u^2v^2 - \frac{9}{16}v^4 + \frac{575}{128}u^5 - \frac{755}{64}u^3v^2 + \frac{435}{128}uv^4 + \ldots\right] \tag{34}$$

From the expansions of T_0 and T_1, the series of T_2 onwards can be obtained using " T_n Eq" shown in Eq. (25). The expansion of T_{n+1} is obtained from the series of T_n and T_{n-1}. Thus, the expansions of T_2, T_3, T_4 and T_5 are given as follows:

$$T_2 = \frac{\pi}{\sqrt{2}}\left[\frac{3}{8}u^2 - \frac{3}{8}v^2 - \frac{9}{8}u^3 + \frac{21}{8}uv^2 + \frac{77}{32}u^4 - \frac{153}{16}u^2v^2 + \frac{37}{32}v^4 - \frac{145}{32}u^5 + \frac{415}{16}u^3v^2 - \frac{285}{32}uv^4 + \ldots\right] \tag{35}$$

$$T_3 = \frac{\pi}{\sqrt{2}}\left[\frac{5}{16}u^3 - \frac{15}{16}uv^2 - \frac{5}{4}u^4 + \frac{105}{16}u^2v^2 - \frac{15}{16}v^4 + \frac{835}{256}u^5 - \frac{3295}{128}u^3v^2 + \frac{2655}{256}uv^4 + \ldots\right] \tag{36}$$

$$T_4 = \frac{\pi}{\sqrt{2}}\left[\frac{35}{128}u^4 - \frac{105}{64}u^2v^2 + \frac{35}{128}v^4 - \frac{175}{128}u^5 + \frac{805}{64}u^3v^2 - \frac{735}{128}uv^4 + \ldots\right] \tag{37}$$

$$T_5 = \frac{\pi}{\sqrt{2}}\left[\frac{63}{256}u^5 - \frac{315}{128}u^3v^2 + \frac{315}{256}uv^4 + \ldots\right] \tag{38}$$

It is to be noted that while Eq. (13) does not include U_0 term it can be formally considered to be zero as can be seen by substitution

of $n = 0$ in Eq. (12) gives $U_0 = 0$.

The series of U_1 is obtained using " U_1 Eq" given in Eq. (23). In this relation the series of T_0 shown in Eq. (33) is substituted to obtain the following:

$$U_1 = \frac{\pi}{\sqrt{2}}\left[\frac{1}{2}v - \frac{3}{2}uv + \frac{51}{16}u^2v - \frac{9}{16}v^3 - \frac{95}{16}u^3v + \frac{45}{16}uv^3 + \frac{1335}{128}u^4v - \frac{555}{64}u^2v^3 + \frac{75}{128}v^5 + \ldots\right] \quad (39)$$

From the expressions of U_0 and U_1, now the series of U_2 onwards can be obtained using " U_n Eq" shown in Eq. (26). The expansion of U_{n+1} is obtained from the series of U_n and U_{n-1}. Thus, the expansions of U_2, U_3, U_4 and U_5 are given as follows:

$$U_2 = \frac{\pi}{\sqrt{2}}\left[\frac{3}{4}uv - 3u^2v + \frac{3}{4}v^3 + \frac{125}{16}u^3v - \frac{85}{16}uv^3 - \frac{135}{8}u^4v + \frac{335}{16}u^2v^3 - \frac{25}{16}v^5 + \ldots\right] \quad (40)$$

$$U_3 = \frac{\pi}{\sqrt{2}}\left[\frac{15}{16}u^2v - \frac{5}{16}v^3 - \frac{75}{16}u^3v + \frac{65}{16}uv^3 + \frac{3705}{256}u^4v - \frac{2945}{128}u^2v^3 + \frac{485}{256}v^5 + \ldots\right] \quad (41)$$

$$U_4 = \frac{\pi}{\sqrt{2}}\left[\frac{35}{32}u^3v - \frac{35}{32}uv^3 - \frac{105}{16}u^4v + \frac{385}{32}u^2v^3 - \frac{35}{32}v^5 + \ldots\right] \quad (42)$$

$$U_5 = \frac{\pi}{\sqrt{2}}\left[\frac{315}{256}u^4v - \frac{315}{128}u^2v^3 + \frac{63}{256}v^5 + \ldots\right] \quad (43)$$

Thus the series of every toroidal harmonic can be obtained from the series T_0 and the relations given in Eqs (23)–(26). In order to obtain the expansion of T_1 from T_0, " T_1 Eq" is used. Once the expansion of T_1 is acquired, the expansion of T_2 can be obtained using " T_n Eq". Proceeding this way, the expansion of T_n can be obtained using " T_n Eq" from the expansions of T_{n-2} and T_{n-1}. The expansion of U_1 can be obtained from the expansion of T_0 using " U_1 Eq". The expansion of U_2 can be obtained from $U_0 = 0$ and expansion of U_1 using " U_n Eq". In this way, the expansion of U_n can be obtained using " U_n Eq" from the expansions of U_{n-2} and U_{n-1}. Thus, the expansions of all harmonics can be obtained using expansion of T_0 alone.

Using the arbitrary precision facility provided by the Java platform, a program was developed for obtaining the power series expansions for any toroidal harmonic (T_n or U_n) up to the desired number of terms.

The expansions presented in this paper were also verified with Mathematica till the fourth degree for T_0, T_1, T_2, T_3, T_4, U_1, U_2, U_3, and U_4.

It was observed that the leading degree terms (lowest degree terms) in the power series expansions of T_n and U_n are real and imaginary parts of $\frac{\pi}{\sqrt{2}}\frac{1}{2}\frac{3}{4}\frac{5}{6}\ldots\frac{2n-1}{2n}(u+iv)^n$ respectively.

3.5. Power series expansion for describing the potential inside a toroidal ion trap

The power series expansion of the potential Ψ shown in Eq. (13) for an arbitrary toroidal trap is presented in this section. It is obtained from the power series of toroidal harmonics T_n and U_n in that equation.

Since Ψ in Eq. (13) is a linear combination of toroidal harmonics and each of the individual toroidal harmonics can be expressed as a power series, Ψ too can be expressed as power series. Ψ can be expressed as

$$\Psi(\rho,\varphi,z) = \alpha_{00} + \alpha_{10}u + \alpha_{01}v + \alpha_{20}u^2 + \alpha_{11}uv + \alpha_{02}v^2 + \alpha_{30}u^3 + \alpha_{21}u^2v + \alpha_{12}uv^2 + \alpha_{03}v^3 + \alpha_{40}u^4 + \alpha_{31}u^3v + \alpha_{22}u^2v^2 + \alpha_{13}uv^3 + \alpha_{04}v^4 + \ldots \quad (44)$$

where α_{ij} 's are given by $\alpha_{00} = \frac{\pi}{\sqrt{2}}a_0$, $\alpha_{10} = \frac{\pi}{\sqrt{2}}\frac{-2a_0+a_1}{2}$, $\alpha_{01} = \frac{\pi}{\sqrt{2}}\frac{b_1}{2}$, $\alpha_{20} = \frac{\pi}{\sqrt{2}}\frac{10a_0-8a_1+3a_2}{8}$, $\alpha_{11} = \frac{\pi}{\sqrt{2}}\frac{3}{4}b_2$, $\alpha_{02} = -\alpha_{20}$, … $\alpha_{13} = \frac{\pi}{\sqrt{2}}\frac{5}{32}(-34b_2 + 26b_3 - 7b_4)$, …

3.6. Equations of ion motion in the toroidal ion trap

The equations of ion motion in an arbitrary toroidal ion trap is derived using fourth degree polynomial approximation to the potential as discussed in Section 3.5.

The time-varying potential in the toroidal ion trap is given in terms of Ψ shown in Eq. (44), by:

$$\Phi(\rho,\varphi,z,t) = \left(U_{dc} + V_{rf}\cos(\Omega t)\right)\Psi(\rho,\varphi,z) \quad (45)$$

where U_{dc} is the d.c. potential, V_{rf} is the r.f. potential and Ω is angular frequency of the r.f. drive.

The time-varying electric field along the ρ-direction is $\frac{\partial\Phi(\rho,\varphi,z,t)}{\partial\rho}$ and it is given by:

$$E_\rho = \frac{1}{2a}\left(U_{dc} + V_{rf}\cos(\Omega t)\right)\left[2\alpha_{20}u + \alpha_{11}v + 3\alpha_{30}u^2 + 2\alpha_{21}uv + \alpha_{12}v^2 + 4\alpha_{40}u^3 + 3\alpha_{31}u^2v + 2\alpha_{22}uv^2 + \alpha_{13}v^3\right] \quad (46)$$

Once E_ρ is obtained the x-direction field can be obtained using $E_x = E_\rho \cos\varphi$ and the y-direction field using $E_y = E_\rho \sin\varphi$, where φ is the angle between the x-axis and the line ON as shown in Fig. 2.

Similarly the z-direction field is $\frac{\partial\Phi(\rho,\varphi,z,t)}{\partial z}$ and it is given by:

$$E_z = \frac{1}{2a}\left(U_{dc} + V_{rf}\cos(\Omega t)\right)\left[\alpha_{11}u + 2\alpha_{02}v + \alpha_{21}u^2 + 2\alpha_{12}uv + 3\alpha_{03}v^2 + \alpha_{31}u^3 + 2\alpha_{22}u^2v + 3\alpha_{13}uv^2 + 4\alpha_{04}v^3\right] \quad (47)$$

Thus the equations of ion motion in the Cartesian coordinate system are given by:

$$m\frac{d^2x}{dt^2} = -eE_x \quad (48)$$

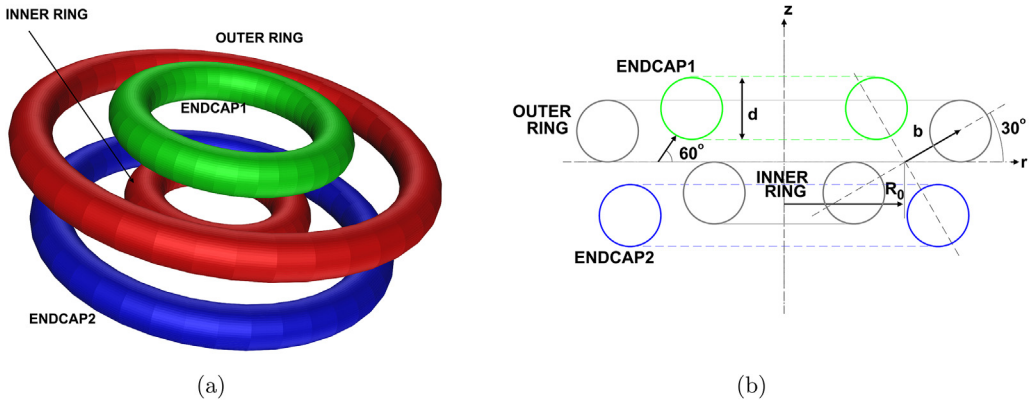

Fig. 4. Schematic view of CircRodTorTrap30. (a) Three dimensional view and (b) cross section in *rz*-plane [5].

$$m\frac{d^2y}{dt^2} = -eE_y \tag{49}$$

$$m\frac{d^2z}{dt^2} = -eE_z \tag{50}$$

where m is mass of the ion and e is charge of the ion.

4. Results and discussions

In this section, the verification of the theory developed in this paper will be carried out using an arbitrary toroidal ion trap geometry. Two simulations will be presented. First of these is the potential within the trapping region predicted by the power series. Second is the trajectory of an ion inside the trap. Both these simulations will be compared with corresponding results obtained using the BEM.

4.1. Geometry and geometry parameters of the trap considered for verification

The geometry considered is CircRodTorTrap30 [5].[3] Schematic view of this trap is shown in Fig. 4. Fig. 4(a) shows the three dimensional view of the trap. Its cross-section in the *rz*-plane is shown in Fig. 4(b). This trap is made up of four electrodes of different diameters. This geometry was formed such that the line joining the centers of ring electrodes on the *rz*-plane subtends 30° with the radial plane and the line joining the centers of endcap electrodes is perpendicular to the line joining the centers of ring electrodes. In this diagram the label R_0 refers to the distance from the origin to the mid-point between ring electrodes on the *r*-axis, b indicates half-distance between the centers of the ring electrodes, and d is diameter of the rods. The values of R_0, b and d are taken to be 40 mm, 20 mm, and 20 mm respectively.

CircRodTorTrap30 was chosen for verification on account of its lack of top-bottom symmetry.

4.2. Coefficients of the power series

To obtain potentials within the trap using the power series developed in this study, it is necessary to first evaluate the coefficients, α_{ij}, of the power series. This section presents the values of these coefficients which have been obtained for CircRodTorTrap30.

To compute the values of α_{ij}, the trapping point (a, z_c) in the *rz*-plane and its toroidal multipole coefficients are required. These are computed using the method outlined in Section 2.4.

The radius of its trapping circle, a, was computed as 39.544313 mm and the trapping height from the radial plane, z_c, was computed to be −0.00329 mm. The non zero value of z_c is due to the stronger effect of the outer ring electrode on the trapping potential than the inner ring [5].

Having obtained the trapping circle, the toroidal multipole coefficients are next computed. This was done by the method outlined in Section 2.4. The values computed for the coefficients a_0, a_1, a_2, a_3, a_4, b_2, b_3, and b_4 are given in Table 1.

Once the multipole coefficients have been computed these can be used for obtaining the values of the coefficients of the power series. The computed values for α_{20} , α_{11}, α_{30}, α_{21}, α_{12}, α_{03}, α_{40}, α_{31}, α_{22}, α_{13}, and $\alpha_{04}$are given in Table 2.

4.3. Comparison of potential obtained using the power series with those obtained using the BEM

In this section potential obtained from the power series will be compared with the potential computed using the BEM. This is done along the radial axis for CircRodTorTrap30 shown in Fig. 4.

Fig. 5(a) compares the potential obtained using power series with the potential computed using the BEM. In this plot on *x*-axis radial distance and on *y*-axis potential are shown. The potential computed using the BEM is plotted as a black continuous line. The potential obtained from the power series (Eq. (44)) with quadratic, cubic, fourth order and fifth order terms have also been plotted using dots. Since the curves overlap, the errors are plotted in Fig. 5(b).

Fig. 5(b) compares the error in the potential due to power series approximation in CircRodTorTrap30. In this plot, *x*-axis indicates radial distance. *y*-axis plots the error in potential. This error refers to the difference between the potential computed using the BEM and the potential obtained from the power series (Eq. (44)). The error due to quadratic, cubic, fourth order and fifth order power series approximation are shown. It can be seen from the figure that the error due to quadratic approximation is small in the range 37 mm and 42 mm, and it is only outside this range the magnitude of the error starts growing. The error due to cubic, fourth order and fifth order approximation are small in the wider range 35 mm and 45 mm.

In summary, the power series provides good approximation to

[3] There was an error in reporting the dimensions of the trap shown in Fig. 4 (CircRodTorTrap30) in Ref. [5].The dimensions that were actually used in those simulations are those that are used in the present study.

Table 1
Toroidal multipole coefficients for the trap CircRodTorTrap30.

a_0	a_1	a_2	a_3	a_4	b_2	b_3	b_4
−0.000721	−0.001442	18.592466	53.108670	91.386469	32.216382	91.642007	179.554871

Table 2
Values of α_{ij} for trap CircRodTorTrap30. All values are dimensionless.

α_{ij}	$j = 0$	$j = 1$	$j = 2$	$j = 3$	$j = 4$
$i = 0$	−0.001602	0	−15.489479	−9.942817	−7.336626
$i = 1$	0	53.675106	−2.180838	10.569577	
$i = 2$	15.489479	−23.846654	46.200596		
$i = 3$	−9.599373	41.111596			
$i = 4$	7.425907				

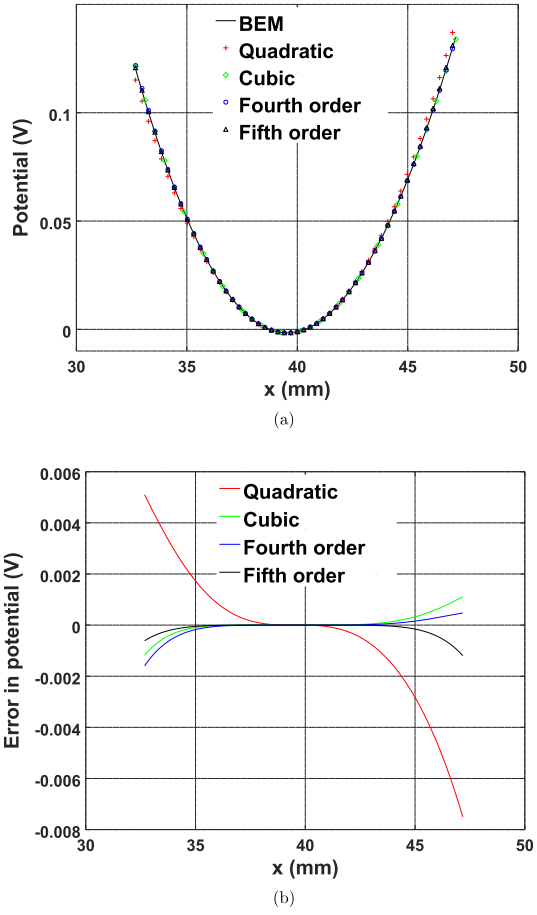

Fig. 5. (a) Comparison of potential obtained from power series with the BEM in radial direction and (b) error in radial direction potential due to power series approximation.

the potential inside the trap.

4.4. Comparison of trajectory obtained using the power series with those obtained using the BEM

In this section trajectory obtained from the power series is compared with the trajectory computed using the BEM.

In the computations of trajectory, the frequency of the r.f. drive is taken as 1 MHz. The r.f. potential was taken to be 805.2953 V_{0-p}, corresponding to a q_z value which was fixed at 0.5 (see Section 2.5). The d.c. potential was kept at zero. The mass to charge ratio of the ion is considered as 78 Th. The step size used in the numerical computation of the trajectory is 10 ns. The comparison of the trajectories was done for 0.1 m s. Initially, the ion was kept on the trapping circle in the xz-plane with velocity in the x-direction as 500m s^{-1}, and in the z-direction as 500m s^{-1}. The initial velocity in the y-direction was kept at 0m s^{-1}, by choice, to restrict the motion to the xz-plane only.

Fig. 6 compares the trajectories obtained by the BEM with those obtained by the power series. The trajectories obtained from the power series are the numerical solutions of the differential equations Eqs. (48)–(50). Also, errors in the trajectories are shown in the same figure. In these figures, time is shown on the x-axis and amplitude on the y-axis.

Fig. 6(a) and (b) compare the amplitudes of ion motion in the x and z direction respectively. It can be seen from the figure that the match between the BEM trajectory and the power series trajectory is good.

Fig. 6(c) and (d) are error plots for the x and z direction amplitudes, respectively. For the x-direction, the error is initially 0 mm and it grows with time. Finally, it reaches its maximum 0.00028 mm around 0.98 m s. For the y-direction, the error is initially 0 mm and it grows with time. Finally, it reaches its maximum 0.000125 mm around 0.095 m s. However, these errors are small in comparison with the amplitude of ion motion.

In summary the power series provides a good approximation for computing trajectories inside toroidal ion trap.

In this study a comparison of potential and ion trajectory obtained from power series with the BEM simulations has been carried out for one toroidal trap. However, several other geometries have also been tested. In these geometries too the potential and trajectory predicted by power series have been compared with those obtained from the BEM. These geometries include one studied by Church [7], two studied by Lammert et al. [1], and one by Taylor and Austin [8]. Additionally, a random geometry proposed in Ref. [5] has also been investigated. In all these five geometries the prediction of the power series for the potential and trajectory had a good match with that obtained by the BEM. The results of these five geometries are not included in this paper for the sake of brevity.

4.5. Use of power series for predicting trap performance: nonlinear resonance at $q_z = 0.78$ in CircRodTorTrap0

Multipole expansions have been used in point trapping devices to provided insight into different aspects of trap performance. These have been briefly alluded to in the Introduction. With the successful implementation of power series for describing potential in toroidal ion traps as presented in this paper, in these traps too the power series can be used to provide useful insight into the dynamics of ions. As an example, the nonlinear resonance at $q_z = 0.78$ [20] in CircRodTorTrap0 (Fig. 7) [5] has been taken up for investigation.

Three dimensional view of CircRodTorTrap0 is shown in Fig. 7(a). Cross-sectional view in rz-plane with trap parameters is shown in Fig. 7(b). The values of parameters R_0, d and b are taken to

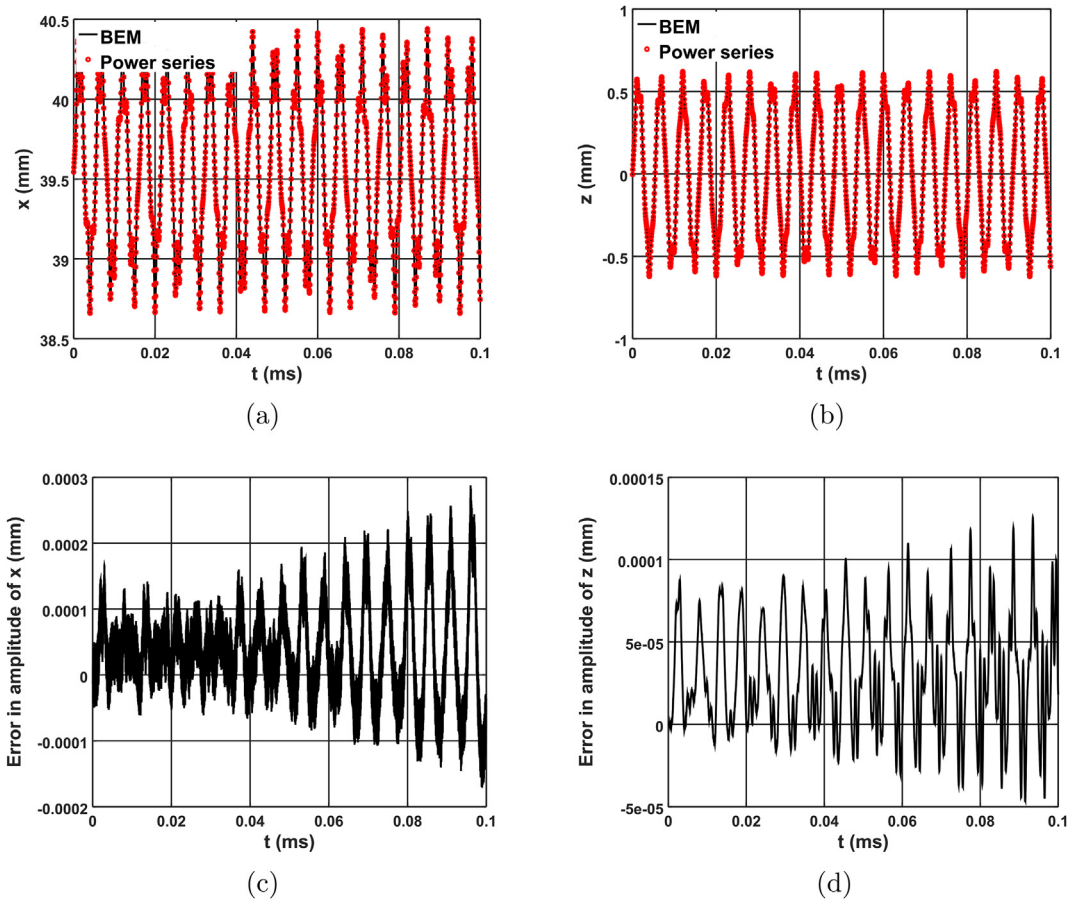

Fig. 6. Comparison of ion trajectories obtained using the BEM simulations (BEM) and power series (Approximate) for CircRodTorTrap30. (a) *x*-direction trajectory, (c) error in *x*-direction trajectory, (b) *z*-direction trajectory and (d) error in *z*-direction trajectory.

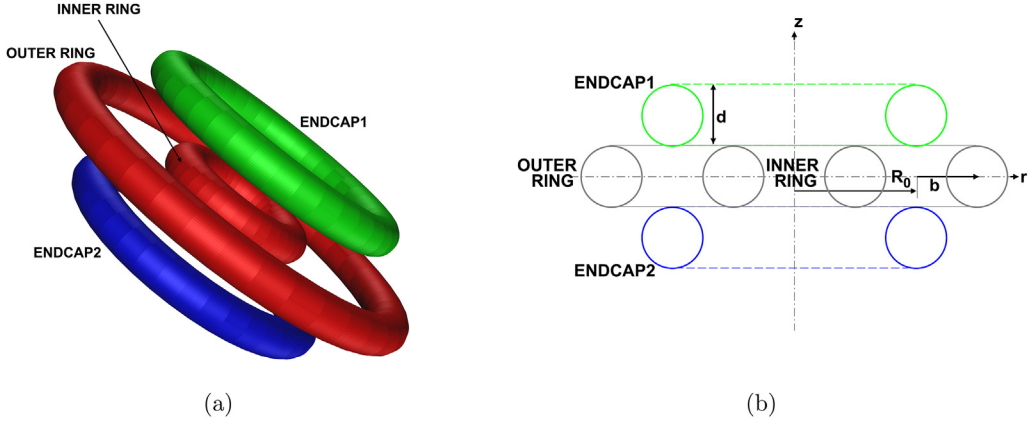

Fig. 7. Schematic view of CircRodTorTrap0. (a) Three dimensional view and (b) cross section in *rz*-plane [5].

be 40 mm, 20 mm, and 20 mm respectively.

In order to check if the theory developed in this paper is capable of predicting the $q_z = 0.78$ nonlinear resonance, the following method is used. Using the toroidal multipoles, the coefficients in the power series are first determined. If the coefficients have nonzero cubic terms then the trap will have nonlinear resonance at $q_z = 0.78$. Next the applied potentials are computed using the quadratic term to ensure $q_z = 0.78$ (see Section 2.5). Using this potential and the computed coefficients the trajectory of ion motion are computed. These trajectories are compared with the trajectories obtained using the BEM under the same conditions. When both trajectories display unstable motion it can be concluded that the power series developed in this paper is capable of predicting nonlinear resonance at $q_z = 0.78$.

In the computation of trajectory, the frequency of the r.f. drive is taken as 1 MHz. The mass to charge ratio of the ion is taken to be 78 Th. The r.f. potential was computed to be 1256.2389 V_{0-p}, corresponding to $q_z = 0.78$ (see Section 2.5). The d.c. potential was kept at zero. The step size used in the numerical computation of the trajectory is 10 ns. The comparison of the trajectory was done for

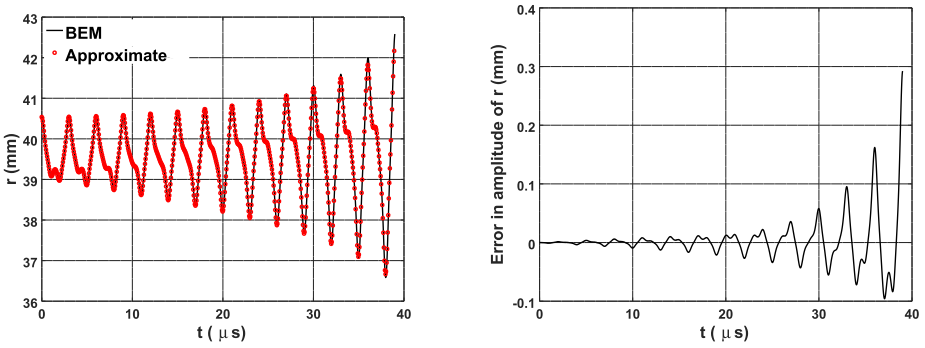

(a) (b)

Fig. 8. Comparison of ion trajectories obtained using the BEM simulations (BEM) and power series (Approximate) for CircRodTorTrap0. (a) Radial motion and (b) error in radial motion.

40 μs. The initial position of ion is 1 mm away from the trapping circle along the radial direction and velocity is taken to be zero.

Fig. 8 compares radial direction trajectory obtained by the BEM with that obtained by the power series. Also, error in the trajectory is shown in the same figure. In this figure, time is shown on the x-axis and amplitude on the y-axis.

Fig. 8(a) shows comparison of amplitude in the radial motion of the ion. The match between approximate solution obtained using power series and the BEM solution is seen to be good. Also, it can be seen that the amplitude of ion motion grows with time. The growth in amplitude of ion motion is captured very well by the power series too.

Fig. 8(b) shows error in the amplitude of ion motion in radial direction. It can be seen from the figure that although the error grows with time, it is still small in comparison to the amplitude of ion motion.

5. Concluding remarks

In this paper, a power series expansion for toroidal harmonics in terms of the radial and axial distances from the trapping circle has been developed. In order to obtain the power series expansion of the individual toroidal harmonics, three-term recurrence relations involving toroidal harmonics of order $n-1$, n, $n+1$ and derivative of toroidal harmonic of order n were obtained. Using these three-term recurrence relations a systematic procedure (in Section 3.4) to obtain the power series of any toroidal harmonic T_n or U_n from the expansion of the lowest harmonic T_0 was presented. This procedure was implemented in the Java platform to obtain expansions of a toroidal harmonic of arbitrary order up to the desired number of terms in the expansion.

To verify the theory developed in this paper, a comparison of potential and ion trajectory obtained from power series with the BEM simulations has been made for one toroidal trap. The agreement between the two is seen to be very good.

Although not discussed here, the three-term recurrence relations derived for toroidal harmonics in this paper are equally valid for toroidal harmonics which have a singularity on the reference circle. The mathematical expressions for such harmonics are obtained by replacing $Q_{n-\frac{1}{2}}(\cosh\tau)$ with $P_{n-\frac{1}{2}}(\cosh\tau)$ in Eqs. (11) and (12). Such harmonics are used in modelling of fields due to magnetic coils [43] and gravitational fields [44].

Finally, the utility of power series to predict trap performance has been demonstrated by the study of the $q_z = 0.78$ nonlinear resonance. In a similar way, the power series could also be used to study ion dynamics in the vicinity of the trapping circle of toroidal ion traps.

Acknowledgements

The authors thank Professor A. G. Menon for discussions during the preparation of this manuscript. The authors thank Ms. Geethanjali Monto for copy-editing the manuscript. We thank two anonymous reviewers of an earlier version of this manuscript for their insightful suggestions.

Appendix B. Supplementary data

Supplementary data to this article can be found online at https://doi.org/10.1016/j.ijms.2019.116261.

Appendix A. Recurrence relations for the toroidal harmonics

Appendix A.1. Generation of new solutions from existing ones for the axially symmetric Laplace equation

Two ways of creating new axially symmetric solutions of the Laplace equation from an existing axially symmetric solution are presented here.

It is to be noted that the potential $W(\rho,z)$ in the cylindrical coordinate system due to an axially symmetric ion trap satisfies the Laplace equation as given below:

$$\frac{\partial^2 W}{\partial \rho^2}+\frac{1}{\rho}\frac{\partial W}{\partial \rho}+\frac{\partial^2 W}{\partial z^2}=0 \tag{A.1}$$

If $W(\rho,z)$ is a solution of A.1 then $W(\rho,z+h)$ will also be a solution for any constant h. The linear combination $\frac{W(\rho,z+h)-W(\rho,z)}{h}$ is also a solution to A.1. As h approaches zero, this quantity approaches $\frac{\partial W}{\partial z}$, which is a new a solution to A.1. Thus it is possible to create a new solution of the axially symmetric Laplace equation (A.1) by simple partial differentiation with respect to z.

It can be shown easily that if $W(\rho,z)$ is a solution to axially symmetric Laplace equation given in A.1, then $W(k\rho,kz)$ is also solution for constant values of k. Also, the linear combination $\frac{W(k\rho,kz)-W(\rho,z)}{k-1}$ is solution. In this considering $k=1+\varepsilon$ (ε is very small number) and taking the limit as ε approaches zero, this is also solution to axially symmetric Laplace equation and is given by $\rho\frac{\partial W}{\partial \rho}+z\frac{\partial W}{\partial z}$. From this, it can be concluded that the application of $\rho\frac{\partial}{\partial \rho}+z\frac{\partial}{\partial z}$ to an existing solution of axially symmetric Laplace equation gives newer solutions.

To summarize, both the $\frac{\partial}{\partial z}$ operator and the $\rho\frac{\partial}{\partial \rho}+z\frac{\partial}{\partial z}$ operator create new axially symmetric solutions of Laplace equation from an existing axially symmetric solutions.

Appendix A.2. Recurrence relations

Since each toroidal harmonic is a solution to the axially symmetric solution Laplace equation, by applying the operators $\frac{\partial}{\partial z}$ or $\left(\rho\frac{\partial}{\partial\rho}+z\frac{\partial}{\partial z}\right)$ a new axially symmetric solution to the Laplace equation is obtained. This new solution is a linear combination of the toroidal harmonics. It turns out that each new solution is expressible as a linear combination of no more than three toroidal harmonics.

Using the steps which are presented in the Supplementary Material, the following novel recurrence relations are obtained.

$$\frac{\partial T_0}{\partial z} = -\frac{1}{2a}U_1 \tag{A.2}$$

$$\left(\rho\frac{\partial}{\partial\rho}+z\frac{\partial}{\partial z}\right)T_0 = -\frac{1}{2}(T_0+T_1) \tag{A.3}$$

$$\frac{\partial T_n}{\partial z} = -\frac{n-\frac{1}{2}}{2a}U_{n-1}+\frac{n}{a}U_n-\frac{n+\frac{1}{2}}{2a}U_{n+1} \tag{A.4}$$

$$\left(\rho\frac{\partial}{\partial\rho}+z\frac{\partial}{\partial z}\right)T_n = \frac{n-\frac{1}{2}}{2}T_{n-1}-\frac{T_n}{2}-\frac{n+\frac{1}{2}}{2}T_{n+1} \tag{A.5}$$

$$\frac{\partial U_n}{\partial z} = \frac{n-\frac{1}{2}}{2a}T_{n-1}-\frac{n}{a}T_n+\frac{n+\frac{1}{2}}{2a}T_{n+1} \tag{A.6}$$

$$\left(\rho\frac{\partial}{\partial\rho}+z\frac{\partial}{\partial z}\right)U_n = \frac{n-\frac{1}{2}}{2}U_{n-1}-\frac{U_n}{2}-\frac{n+\frac{1}{2}}{2}U_{n+1} \tag{A.7}$$

References

[1] L.A. Lammert, W.R. Plass, C.V. Thompson, M.B. Wise, Design, optimization and initial performance of a toroidal rf ion trap mass spectrometer, Int. J. Mass Spectrom. 212 (2001) 25–40.
[2] R.E. March, Quadrupole Ion Traps. Mass Spectrometry Reviews, vol. 28, Wiley Periodicals, Inc., 2009, pp. 961–989.
[3] G. Wu, R.G. Cooks, Z. Ouyang, Geometry optimization for the cylindrical ion trap: field calculations, simulations and experiments, Int. J. Mass Spectrom. 241 (2005) 119–132.
[4] M.E. Bier, J.E.P. Syka, Ion Trap Mass Spectrometer System and Method, U.S. Patent No. 5420425 A., 1995.
[5] Appala Naidu Kotana, Atanu K. Mohanty, Determination of multipole coefficients in toroidal ion trap mass analysers, Int. J. Mass Spectrom. 408 (2016) 62–76.
[6] S.A. Lammert, A.A. Rockwood, M. Wang, M.L. Lee, E.D. Lee, S.E. Tolley, J.R. Oliphant, J.L. Jones, R.W. Waite, Miniature toroidal radio frequency ion trap mass analyzer, J. Am. Soc. Mass Spectrom. 17 (2006) 916–922.
[7] D.A. Church, Storage ring ion trap derived from the linear quadrupole radio frequency mass filter, J. Appl. Phys. 40 (1969) 3127–3134.
[8] N. Taylor, D.E. Austin, A simplified toroidal ion trap mass analyzer, Int. J. Mass Spectrom. 321 (2012) 25–32.
[9] M. Wang, H.E. Quist, B.J. Hansen, Y. Peng, Z. Zhang, A.R. Hawkins, A.L. Rockwood, D.E. Austin, M.L. Lee, Performance of a halo ion trap mass analyzer with exit slits for axial ejection, J. Am. Soc. Mass Spectrom. 22 (2011) 369–378.
[10] J.A. Contreras, J.A. Murray, S.E. Tolley, J.L. Oliphant, H.N. Tolley, S.A. Lammert, E.D. Lee, D.W. Later, M.L. Lee, Hand-portable gas chromatograph-toroidal ion trap mass spectrometer (gc-tms) for detection of hazardous compounds, J. Am. Soc. Mass Spectrom. 19 (2008) 1425–1434.
[11] D.E. Austin, M. Wang, S.E. Tolley, J.D. Maas, A.R. Hawkins, A.L. Rockwood, H.D. Tolley, E.D. Lee, M.L. Lee, Halo ion trap mass spectrometer, Anal. Chem. 79 (2007) 2927–2932.
[12] M.J. Madsen, C.H. Gorman, Compact toroidal ion-trap design and optimization, Phys. Rev. A 82 (2010) 0434231–0434237.
[13] I. Waki, S. Kassner, G. Birkl, H. Walther, Observation of ordered structures of laser cooled ions in a quadrupole storage ring, Phys. Rev. Lett. 68 (1992) 2007–2010.
[14] Y. Peng, B.J. Hansen, H. Quist, Z. Zhang, M. Wang, A.R. Hawkins, D.E. Austin, Coaxial ion trap mass spectrometer: concentric toroidal and quadrupolar trapping regions, Anal. Chem. 83 (2011) 5578–5584.
[15] J.M. Higgs, D.E. Austin, Simulations of ion motion in toroidal ion traps, Int. J. Mass Spectrom. 363 (2014) 40–51.
[16] J.M. Higgs, B.V. Petersen, S.A. Lammert, K.F. Warnick, D.E. Austin, Radio-frequency trapping of ions in a pure toroidal potential distribution, Int. J. Mass Spectrom. 395 (2016) 20–26.
[17] J.M. Higgs, K.F. Warnick, D.E. Austin, Field optimization of toroidal ion trap mass analyzers using toroidal multipoles, Int. J. Mass Spectrom. 425 (10–15) (2018).
[18] Appala Naidu Kotana, Atanu K. Mohanty, Computation of mathieu stability plot for an arbitrary toroidal ion trap mass analyser, Int. J. Mass Spectrom. 414 (2017) 13–22.
[19] S. Lammert, E. Lee, R. Waite, J. Oliphant, D. Austin, J. Higgs, K.F. Warnick, D. Tolley, Toroidal multipole expansion for the design of circular ion traps, in: 62ndASMS Conference on Mass Spectrometry and Allied Topics, 2014.
[20] Ailin Li, J.M. Higgs, D.E. Austin, Chaotic motion of single ions in a toroidal ion trap mass analyzer, Int. J. Mass Spectrom. 425 (2018) 10–15.
[21] E.C. Beaty, Calculated electrostatic properties of ion traps, Phys. Rev. A 33 (1986) 3645–3656.
[22] J.D. Williams, K.A. Cox, R.G. Cooks, S.A. McLuckey, K.J. Hart, D.E. Goerlnger, Resonance ejection ion trap mass spectrometry and nonlinear field contributions: the effect of scan direction on mass resolution, Anal. Chem. 66 (1994) 725–729.
[23] Y. Wang, J. Franzen, The non-linear ion trap. part 3. multipole components in three types of practical ion trap, Int. J. Mass Spectrom. Ion Process. 132 (1994) 155–172.
[24] P.H. Dawson, N.R. Whetten, Non-linear resonances in quadrupole mass spectrometers due to imperfect fields i. the quadrupole ion trap, Int. J. Mass Spectrom. Ion Phys. 2 (01) (1969) 45–59.
[25] N. Rajanbabu, A. Chatterjee, A.G. Menon, Motional coherence during resonance ejection of ions from Paul traps, Int. J. Mass Spectrom. 261 (2007) 159–169.
[26] Y. Wang, J. Franzen, The non-linear resonance quistor part 1. potential distribution in hyperboloidal quistors, Int. J. Mass Spectrom. Ion Process. 112 (1992) 167–178.
[27] Y. Wang, J. Franzen, K.P. Wanczek, The non-linear resonance ion trap. part 2. a general theoretical analysis, Int. J. Mass Spectrom. Ion Process. 124 (1993) 125–144.
[28] J. Franzen, The non-linear ion trap. part 4. mass selective instability scan with multipole superposition, Int. J. Mass Spectrom. Ion Process. 125 (1993) 165–170.
[29] J. Franzen, The non-linear ion trap. part 5. nature of non-linear resonances and resonant ion ejection, Int. J. Mass Spectrom. Ion Process. 130 (1994) 15–40.
[30] N. Rajanbabu, Amol Marathe, A. Chatterjee, A.G. Menon, Multiple scales analysis of early and delayed boundary ejection in Paul traps, Int. J. Mass Spectrom. 261 (2007) 170–182.
[31] W.R. Plass, Hongyan Li, R.G. Cooks, Theory, simulation and measurement of chemical mass shifts in rf quadrupole ion traps, Int. J. Mass Spectrom. 228 (2003) 237–267.
[32] Xiaoyu Zhou, Caiqiao Xiong, Gaoping Xu, Hao Liu, Yin Tang, Zhiqiang Zhu, Rui Chen, Haoxue Qiao, Yao-Hsin Tseng, Wen-Ping Peng, Zongxiu Nie, Yi Chen, Potential distribution and transmission characteristics in a curved quadrupole ion guide, J. Am. Soc. Mass Spectrom. 22 (2011) 386–398.
[33] David A. Dahl, Simion for the personal computer in reflection, Int. J. Mass Spectrom. 200 (1) (2000) 3–25.
[34] Heui Huang Lee, Finite Element Simulations with ANSYS Workbench 12, pap/dvdr edition, Schroff Development Corp, 2010.
[35] P.K. Tallapragada, A.K. Mohanty, A. Chatterjee, A.G. Menon, Geometry optimization of axially symmetric ion traps, Int. J. Mass Spectrom. 264 (2007) 38–52.
[36] H. William, Press, Saul A. Teukolsky, William T. Vetterling, Brian P. Flannery, Numerical Recipes in C, second ed., Cambridge University Press, Cambridge, USA, 1992.
[37] E. Kreyszig, Advanced Engineering Mathematics, eighth ed., John Wiley & Sons, New York., 1999.
[38] Appala Naidu Kotana, PhD. (Engg.) Thesis, in: Numerical Studies of Axially Symmetric Ion Trap Mass Analysers, Department of Computational and Data Sciences, Indian Institute of Science, Bangalore, India., 2017.
[39] R.E. March, R.J. Hughes, Quadrupole Storage Mass Spectrometry, Wiley-Interscience, New York., 1989.
[40] P.M. Morse, H. Feshbach, Methods of Theoretical Physics, Part I, McGraw-Hill, New York., 1953.
[41] P.M. Morse, H. Feshbach, Methods of Theoretical Physics, Part II, McGraw-Hill, New York., 1953.
[42] M. Abramowitz, I.A. Stegun, Handbook of Mathematical Functions, Dover Publications Inc., New York, 1970.
[43] B.Ph van Milligen, A. Lopez Fraguas, Expansion of vacuum magnetic fields in toroidal harmonics, Comput. Phys. Commun. 81 (1994) 74–90.
[44] Toshio Fukushima, Zonal toroidal harmonic expansions of external gravitational fields for ring-like objects, Astron. J. 152 (2016) 35.